Optimization of Green Hydrogen Production in an Alkaline Electrolyzer

Maria Gabriela Chagas de Oliveira[1], Caio Vinicius Pinheiro Vital[1] and Luis Arturo Gómez-Malagón[1]

[1] University of Pernambuco, Polytechnic School of Pernambuco, 50720-001, Recife, PE, Brazil.

Abstract

Green hydrogen production via alkaline water electrolysis is a key pathway for decarbonizing the energy sector, offering advantages in cost and scalability. This study presents an optimization methodology for a photovoltaic-powered alkaline electrolyzer system to maximize annual hydrogen production. The system integrates a single-diode model for the photovoltaic (PV) panel with an electrochemical model for the electrolyzer, accounting for temperature-dependent performance characteristics. Using Particle Swarm Optimization (PSO), the operational parameters of temperature and number of electrolytic cells were optimized under realistic meteorological conditions. Irradiance data throughout the year 2023 were obtained for the city of Recife-PE using the PVGIS (Photovoltaic Geographical Information System) tool. For the proposed model, results shown that optimal configuration of 7 cells operating at 80°C maximizes annual hydrogen yield. Higher temperatures significantly enhance production rates, though this must be balanced against the energy requirements for temperature maintenance. This research provides valuable insights into operational parameter optimization a solar-driven green hydrogen production system.

Keywords: Green Hydrogen, Alkaline Electrolysis, Optimization, Temperature Control, Electrolytic Cells, Hydrogen Production.

1. Introduction

The growing energy demand driven by urban expansion, industrial development, transportation consumption, and other factors makes the pursuit of a greater diversity of sources essential for ensuring global energy security. On the other hand, the events generated by climate change make the reduction of carbon emissions a global necessity, thereby increasing the demand for renewable energy (IEA, 2025). However, for this transition to be feasible, it is crucial to ensure a constant energy supply. This is necessary so that the intermittency of certain renewable sources, such as solar and wind, does not become an obstacle to reducing reliance on fossil fuels (Baquero and Monsalve, 2024). The use of hydrogen as an energy vector has been widely discussed, as it can be stored, distributed, and converted into electrical energy through fuel cells, thereby compensating for the intermittency of certain sources (Kovač et al, 2021). For hydrogen to be considered clean, it must be produced without carbon emissions. The color-based classification is directly linked to its production method. Notably, black hydrogen, produced through coal gasification, has high carbon emissions, while gray hydrogen, obtained via steam methane reforming without carbon capture, results in high CO_2 emissions. In contrast, blue hydrogen, also produced via steam methane reforming but with carbon capture, features low CO_2 emissions. Turquoise hydrogen, produced through methane pyrolysis with solid carbon storage, generates no direct carbon emissions, and green hydrogen, produced from renewable sources, also results in no direct emissions (Incer-Valverde et al, 2023).

Although most hydrogen today is still produced from fossil fuels, due to the high costs of clean hydrogen production, the number of projects employing electrolysis, a high-potential decarbonization pathway, is growing (IEA, 2024). Among available technologies, Alkaline Electrolysis (AE) is well established, highly scalable, and more cost-effective than Proton Exchange Membrane (PEM) and Solid Oxide Electrolysis (SOE) (Daoudi and Bounahmidi, 2024). However, this process has its drawbacks, such as corrosion caused by the use of electrolytes, lower efficiency, and limited current density (Jin et al,2025). Although the Power-to-

10.18086/swc.2025.05.10 Available at http://proceedings.ises.org

Hydrogen efficiency ranges from 50% to 65% for AEs, from 65% to 70% for PEM electrolyzers, and from 90% to 95% for SOE Cells, it can be enhanced for AEs optimizing operational variables, such as the number of electrolytic cells, temperature, concentration or electrode distance (Hu et al, 2022) (Emam et al., 2024). Thus, optimization techniques can be applied to identify the ideal combination of these parameters for maximizing hydrogen output. In this study a PV-AE system is modelled and simulated, using optimization methods (Particle Swarm Optimization) to determine the optimal operating temperature and number of electrolytic cells that maximize annual hydrogen production.

2. Methodology

The system was modelled through the current-voltage (I-V) curves of both the photovoltaic panel and the alkaline electrolyzer from models proposed in the literature. The simulation of the system was carried out computationally using Python as the programming language. Then, the optimization problem was formulated to identify the optimal parameters that define the operation point, such as the operating temperature and number of cells, that maximize hydrogen production. The optimization algorithm employed for this purpose was the PSO.

2.1. Modelling

2.1.1. Alkaline Electrolizer

An alkaline electrolyzer consists of two electrodes where voltage is applied in their terminals, and a porous diaphragm, which separates the cathode from the anode, preventing gas mixing during water splitting. An electrolyte, such as KOH or NaOH, is added to the water to enhance ion flow, facilitating the hydrogen and oxygen evolution reactions. A schematic diagram of the AE is presented in Fig. 1:

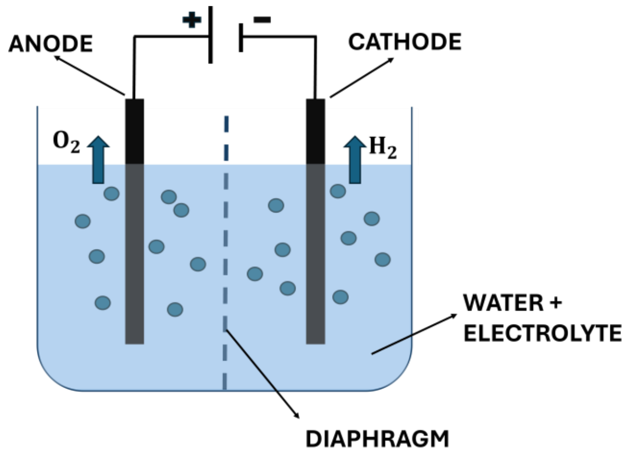

Figure 1: Schematic of an Alkaline Electrolyzer (AE).

The global reaction, shown in equation 1, and the reactions in the cathode and anode, given by equations 2 and 3 (Daoudi and Bounahmidi, 2024) are:

$$Global\ Reaction: \quad H_2O_{(l)} \rightarrow 2H_{2\,(g)} + \frac{1}{2}\,O_2 \qquad \text{(eq. 1)}$$

$$Cathode: \quad 4H_2O_{(l)} + 4e^- \rightarrow 2H_{2\,(g)} + 4OH^- \qquad \text{(eq. 2)}$$

$$Anode: \quad 4OH^-{}_{(aq)} \rightarrow O_{2\,(g)} + 2H_2O_{(l)} + 4e^- \qquad \text{(eq. 3)}$$

A minimum potential difference, known as the Reversible Voltage V_{rev} (V_{rev} in V), must be applied to the cell for these reactions to proceed. This required voltage depends on cell temperature in Kelvin $T_K = T + 273.15$, (T in °C) as given by equation 4 (Stewart et al, 2021):

$$V_{rev} = 1.5184 - 1.5421 \text{ x } 10^{-3} T_K + 9.523 \text{ x } 10^{-5} T_K \ln(T_K) + 9.84 \text{ x } 10^{-8} {T_K}^2 \qquad \text{(eq. 4)}$$

The first electrochemical model to obtain the I-V (I in A and V in V) curve of an alkaline electrolyzer considers the influence of cell temperature T (T in °C) and electrode area A (A in m²), as described by equation 5 (Ulleberg, 2003) as:

$$V = V_{rev} + (r_1 + r_2 T)\frac{I}{A} + s \log\left(\left(t_1 + \frac{t_2}{T} + \frac{t_3}{T^2}\right)\frac{I}{A} + 1\right) \qquad \text{(eq. 5)}$$

where the coefficients s and t are related to the electrode overpotential and the parameter r is associated with the electrolyte resistance. In addition to the cell temperature, several other factors can be incorporated into the modeling of the electrolyzer's I-V curve, such as the distance between the electrodes and the diaphragm, and the electrolyte concentration. Then, equation 5 can be extended by incorporating the parameters p and q, where p accounts for the change in system resistance with electrolyte concentration C (C in M), and q, which represents the variation in resistance with the electrode-diaphragm distance d (d in mm), as expressed in equation 6 (Amores et al, 2014) as:

$$V = V_{rev} + (r_1 + p_1 + q_1 + r_2 T + p_2 C + p_3 C^2 + q_2 d)\frac{I}{A} + s \log\left(\left(t_1 + \frac{t_2}{T} + \frac{t_3}{T^2}\right)\frac{I}{A} + 1\right) \qquad \text{(eq. 6)}$$

The coefficients for both models are determined experimentally and depend on the specific electrolyzer. For this work, the coefficients were adopted from the literature and are listed in Table 1 (Amores et al., 2014).

Table 1: coefficients adopted from literature (Amores et al, 2014).

Coefficients	Units	Values
r_1	$(\Omega\, m^2)$	$3.53855 \text{ x } 10^{-4}$
r_2	$(\Omega\, m^2 °C^{-1})$	$-3.02150 \text{ x } 10^{-6}$
t_1	$(A^{-1} m^2)$	5.13093
t_2	$(A^{-1} m^2 °C)$	$-2.40447 \text{ x } 10^{2}$
t_3	$(A^{-1} m^2 °C)$	$5.99576 \text{ x } 10^{3}$
s	(V)	$2.2396 \text{ x } 10^{-1}$
p_1	$(\Omega\, m^2)$	$3.410251 \text{ x } 10^{-4}$
p_2	$(\Omega\, m^2 M^{-1})$	$-7.489577 \text{ x } 10^{-5}$
p_3	$(\Omega\, m^2 M^{-2})$	$3.916035 \text{ x } 10^{-6}$
q_1	$(\Omega\, m^2)$	$-1.576117 \text{ x } 10^{-4}$
q_2	$(\Omega\, m^2 mm^{-1})$	$1.576117 \text{ x } 10^{-5}$

The density of the KOH electrolyte solution ρ (ρ in kg/m³), as a function of temperature T (T in °C) and KOH weight percentage *wt%,* is given by equation 7 (Stewart et al, 2021), as:

$$\rho = (1002.8 - 0.025T^2 - 0.182T)e^{0.0086wt\%} \qquad \text{(eq. 7)}$$

To obtain the molar concentration C (C in M), equation 8 can be applied, where MM (MM in g/mol) is the molar mass of the electrolyte (Stewart et al, 2021), given by:

$$C = \frac{wt\%}{100}\frac{\rho}{MM} \qquad \text{(eq. 8)}$$

The gas flow rate $\dot{m}_{H_2}$($\dot{m}_{H_2}$ in gm⁻²s⁻¹) produced at the electrode area can be calculated using Faraday's law, according to equation 9 (Stewart et al, 2021), as:

$$\dot{m}_{H_2} = \frac{M_{H_2}}{2F}\frac{I}{A} \qquad \text{(eq. 9)}$$

where M_{H_2} is the molar mass of H_2, F (F = 96465 C mol^{-1}) is the Faraday constant, I (I in A) is the current, and A (A in m^2) is the electrode area (Stewart et al, 2021).

The electrolyzer efficiency $\eta_{electrolyzer}$ is obtained from equation 10 (Stewart et al, 2021), as:

$$\eta_{electrolyzer} = \frac{HHV_{H_2}\,\dot{m}_{H_2}}{V\,\frac{I}{A}} \qquad \text{(eq. 10)}$$

where HHV_{H_2}(HHV_{H_2}= 142000 J g^{-1}) corresponds to the Higher Heating Value of hydrogen (Stewart et al, 2021).

2.1.2. PV panel

The PV panel is modelled using the Single-Diode Model (SDM). The model, used to represent a PV cell electrical behaviour, is represented by an equivalent cicuit composed of a current source in parallel with a diode, a shunt resistance and a series resistance (Tian et al, 2012), as shown in Fig. 2:

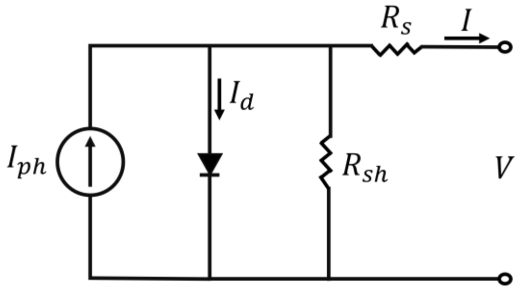

Figure 2: PV cell equivalent circuit (Single-diode model).

The current-voltage relationship, based on Kirchhoff's current law, is given by equation 11 (Tian et al, 2012):

$$I = I_{ph} - I_d\left(e^{\frac{q(V+IR_S)}{nKT_K}} - 1\right) - \frac{V+IR_S}{R_{sh}} \qquad \text{(eq. 11)}$$

where I (I in A) is the cell current, I_{ph} (I_{ph} in A) is the photocurrent, I_d (I_d in A) is the diode saturation current, q is the elementary electron charge (q = 1.602 x 10^{-19} C), K is Boltzmann's constant (K = 1.381 x 10^{-19} J/K), T_K (T_K in K) is the cell temperature, n is the diode ideality factor, R_s (R_s in Ω) is the cell series resistance, R_{sh} (R_{sh} in Ω) is the cell parallel resistance or shunt resistance, V (V in V) is the output voltage.

A photovoltaic module is usually composed of a number N_s of solar cells connected in series. Therefore, equation 11 can be expanded to represent the entire module (Tian et al., 2012), resulting in equation 12:

$$I_M = I_{ph} - I_s\left(e^{\frac{q(V_M+I_M N_S R_S)}{n\,N_S K T_K}} - 1\right) - \frac{V_M+I_M N_S R_S}{N_S R_{sh}} \qquad \text{(eq. 12)}$$

where I_M (I_M in A) is the module output current and V_M (V_M in V) is the module output voltage.

2.2. Optimization algorithm

To maximize the hydrogen production of an electrolyzer, optimization techniques can be employed to determine the parameter combinations that enable optimal generation. Optimization consists of locating global extrema (maximum or minimum) of a function (linear or nonlinear), called an Objective Function. To find the optimum point, certain parameters, called decision variables, can be adjusted to achieve the objective. These variables can be continuous, discrete, or a mixture of both. The Objective Function is subject to constraints, which are rules (equalities and/or inequalities) that must be satisfied by the design variables (Yang, 2008). When an optimization problem involves a nonlinear objective function and constraints, and includes both continuous and discrete variables, it becomes a Mixed Integer Nonlinear Programming (MINLP) problem (Bussieck and Pruessner, 2003).

Optimization algorithms are often inspired by the behavior and decision-making processes of living organisms in nature. The Particle Swarm Optimization (PSO) algorithm was selected due to its ability to handle mixed-integer nonlinear optimization problems (MINLPs) and quick convergence (Fukuyama et al., 2008). PSO algorithm is based on the behavior of bird swarms, where each particle represents a potential solution (Bussieck and Pruessner, 2003). The velocity and position of each particle are updated using equation 13 and equation 14 (Gad, 2022):

$$v_i^{t+1} = wv_i^t + c_1 rand_1(pbest_i - x_i^t) + c_2 rand_2(gbest - x_i^t) \qquad \text{(eq. 13)}$$

and

$$x_i^{t+1} = x_i^t + v_i^{t+1} \qquad \text{(eq. 14)}$$

where v_i^t is the velocity of particle i at iteration t, w is the inertia weight, c_1(cognitive) and c_2 (social) are acceleration coefficients, $rand_1$ and $rand_2$ are random vectors with values between 0 and 1, $pbest_i$ is personal/individual best position of particle i, $gbest$ is global best position and x_i^t is the position vector of particle i at iteration t.

The PSO algorithm operates by finding the best solution through the interaction of a set of particles that converge at specific velocities toward the global optimum, as illustrated in the flowchart of Fig. 3:

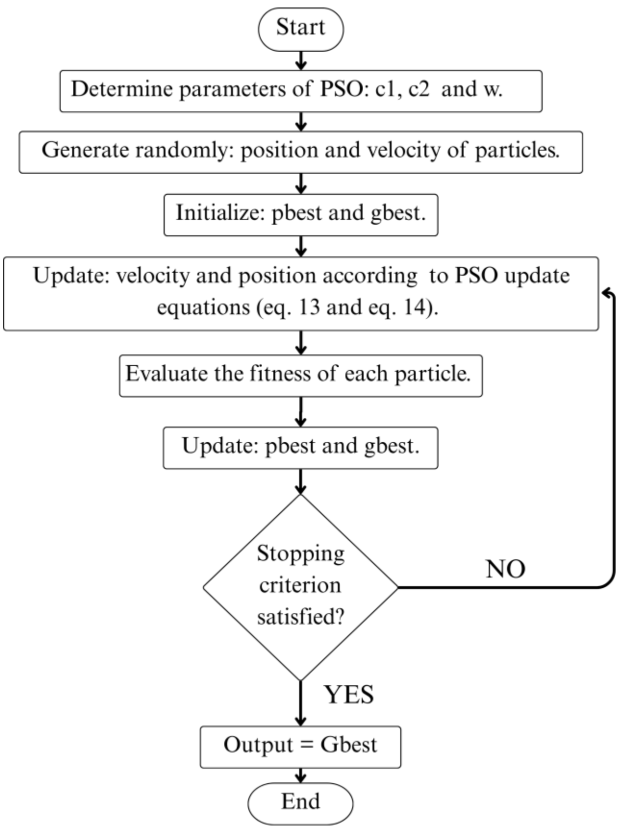

Figure 3: Flowchart of PSO algorithm.

2.3. Simulation

2.3.1. Acquisition of irradiance data

The irradiance and ambient temperature hourly data throughout the year 2023 were obtained for the city of Recife - PE using the PVGIS (Photovoltaic Geographical Information System) tool (European Commission, 2025), based on the PVGIS-SARAH3 database, using the parameters: Latitude (-8.058°), Longitude (-34.885°), Altitude (12 m), Surface tilt (0°) and Azimuth (0°).

2.3.2. Photovoltaic panel

To obtain the I-V curve of the photovoltaic panel considering different irradiance and cell temperature values, an optimization was performed in Python using the PSO algorithm from the pyswarm library to obtain the panel parameters based on the SDM for photovoltaic modules with series-connected cells as shown in equation 12. The I-V curve data points for irradiance at 1000 W/m² and a temperature of 25°C were extracted from the curve provided in the panel's datasheet using WebPlotDigitizer software (Rohatgi, 2024). The optimization aims to find the optimal parameters that minimize the root mean square error (RMSE) between the generated curve and the curve extracted from the datasheet. With the parameters I_{ph}, I_d, R_s, R_{sh} and n, along with the datasheet data, it is possible to obtain the panel's curve and adjust it for different irradiances and temperatures.

2.3.3. Electrolyzer

The I-V curve of the electrolyzer was implemented in Python using equation 6 considering an electrode area A of 0.001 m², a KOH concentration of 32wt% and an electrode-diaphragm distance d of 10 mm (Amores et al, 2014). The reversible voltage and electrolyte density were calculated considering temperature, as shown in equation 4 and equation 7 (Stewart et al, 2021).

2.3.4. Production optimization

The electrolyzer's operating point is determined by the intersection of the PV panel's I-V curve and the electrolyzer's I-V curve. This intersection point can be altered by varying certain parameters, such as: the electrolyzer temperature, which modifies the slope of the electrolyzer's I-V curve; and the number of electrolytic cells in the system, which causes a shift in the electrolyzer's curve. Thus, optimizing these parameters can maximize hydrogen production.

The optimization algorithm was implemented in Python using pandas, numpy, and scipy.optimize libraries. The objective function is to maximize the annual hydrogen production (g/year). Since the hydrogen flow rate is calculated in g/s and the simulation uses hourly irradiance, the annual production is calculated by summing the hourly production (3600 x N_{cells} x hydrogen flow rate) over the entire year. The hydrogen flow rate $\dot{m}_{H_2}$, defined by equation 9, is proportional to the current, but the current I is determined by the intersection of the I-V curves of the PV and the electrolyzer, which constitutes a nonlinear problem. The operational voltage constraint $V_{operational}$ requires $N_{cells}V_{electrolyzer} = V_{PV}$, where V_{PV} and $V_{electrolyzer}$ are both nonlinear functions. The maximum current supported per electrolyzer cell is defined by the operational current $I_{operational}$ of 4 A given by the manufacturer (ElectroCell, 2017) (Amores et al, 2014). The decision variables are the number of electrolytic cells, N_{cells} (an integer variable representing the quantity of series-connected cells in the electrolyzer, characterized as discrete) and operating temperature T (a continuous variable defining the operating temperature of the electrolyzer stack, expressed in degrees Celsius). The problem is a Mixed-Integer Nonlinear Programming (MINLP) problem with two decision variables and a nonlinear objective function.

The established search boundaries were number of electrolyzer cells between 1 and 10 units, and operating temperature between 25°C and 80°C, with 25°C set as the lower limit, corresponding to ambient temperature, and 80°C representing a typical operating temperature for an alkaline electrolyzer based on literature data such as: 65°C – 100°C (El-Shafie, 2023), 70°C – 90°C (Kumar and Lim, 2022).

Then the optimization problem can be formulated as:

Maximize:

$$f(N_{cells}, T) = Annual\ H_2\ production(N_{cells}, T) = \sum 3600\ N_{cells}\ \dot{m}_{H_2}$$

Subject to

$$V_{operational} = V_{PV} = N_{cells} V_{electrolyzer}$$

$$0\ \text{A} < I_{operational} < 4\ \text{A}$$

$$V_{electrolyzer} > V_{rev}$$

$$1 \leq N_{cells} \leq 10$$

$$25°C \leq T \leq 80°C$$

The PSO algorithm was the selected method for the optimization problem, conducted in two sequential stages, with the following parameters:

- First stage: number of particles = 25, maximum iterations = 25, inertia coefficient w = 0.9, cognitive coefficient c_1 = 2.2 and social coefficient c_2 = 1.2;
- Second stage: number of particles = 20, maximum iterations = 20, inertia coefficient w = 0.8, cognitive coefficient c_1 = 2.0 and social coefficient c_2 = 1.4.

3. Results

The solar panel used as an example to obtain electrical characteristics data, as well as to extract the points of it's I-V curve, was the 60 W Ameresco Solar photovoltaic module, model 60J (Ameresco, Inc., 2015). The panel's STC characteristics ensure that the electrolyzer's maximum operating current of 4 A is not exceeded (ElectroCell, 2017). The parameters of the photovoltaic panel, the photocurrent I_{ph} of 3.5390 A, the diode saturation current I_d of 9.3241 x 10^{-10}A, the cell series resistance R_s of 0.0156 Ω, the shunt resistance R_{sh} of 285.6297 Ω and diode ideality factor n of 1.0248, were obtained through optimization as shown in Fig. 4, with a minimum RMSE achieved of 0.0209, considering a reference I-V curve for an irradiance of 1000 W/m².

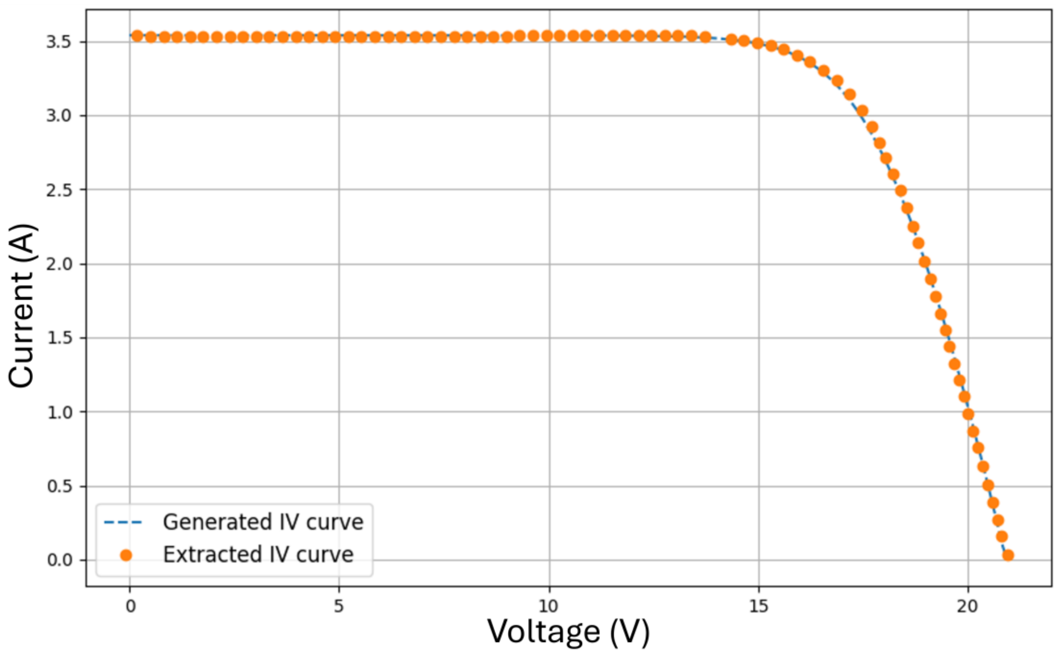

Figure 4: Comparison between PV I-V curves extracted from datasheet generated PV IV curve (with optimal parameters). Dots are experimental values reported by the manufacturer and the line is the single diode model.

The characteristic constants and data of the electrolyzer ELECTROCELL, model Micro Flow Cell, were reproduced from the literature (Amores et al, 2014). The simulation results demonstrate that while temperature variation affects the slope of the electrolyzer's I-V curve, modifying the number of cells shifts its position. Fig.5 shows the behavior of the electrolyzer's I-V curve with varying temperature and number of cells.

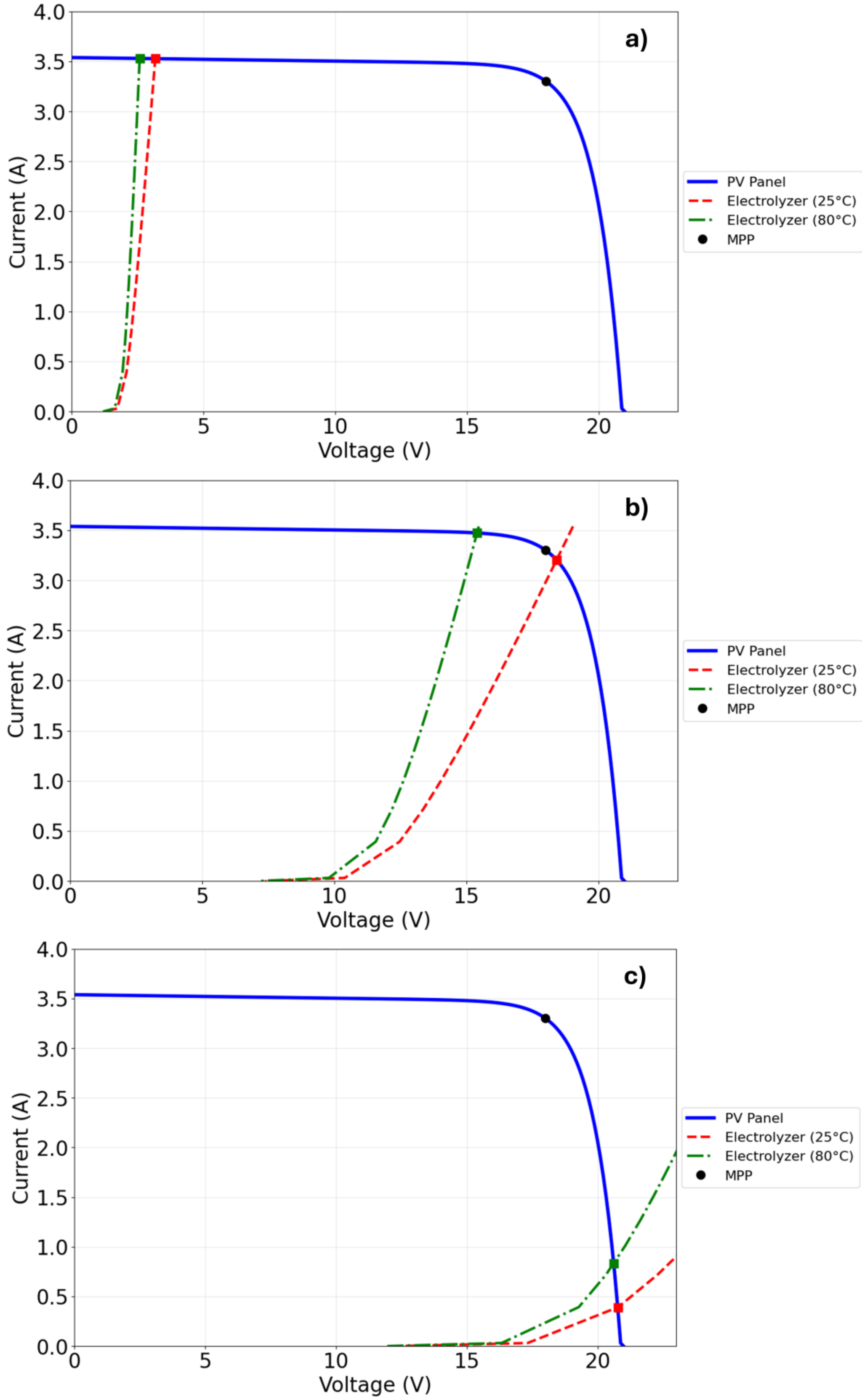

Figure 5: I-V curves of the PV panel (at standard conditions showing the Maximum Power Point (MPP), filled circle in black) and the electrolyzer at 25°C and 80°C for a) 1 cell, b) 6 cells and C) 10 cells.

Irradiance data was obtained throughout the year 2023, collected on an hourly basis, showing high irradiance values at the beginning and at the end of the year, and a decrease in the middle of the year. This mid-year period corresponds to winter, which is typically characterized by a higher frequency of rainy and cloudy days, as shown in Fig. 6.

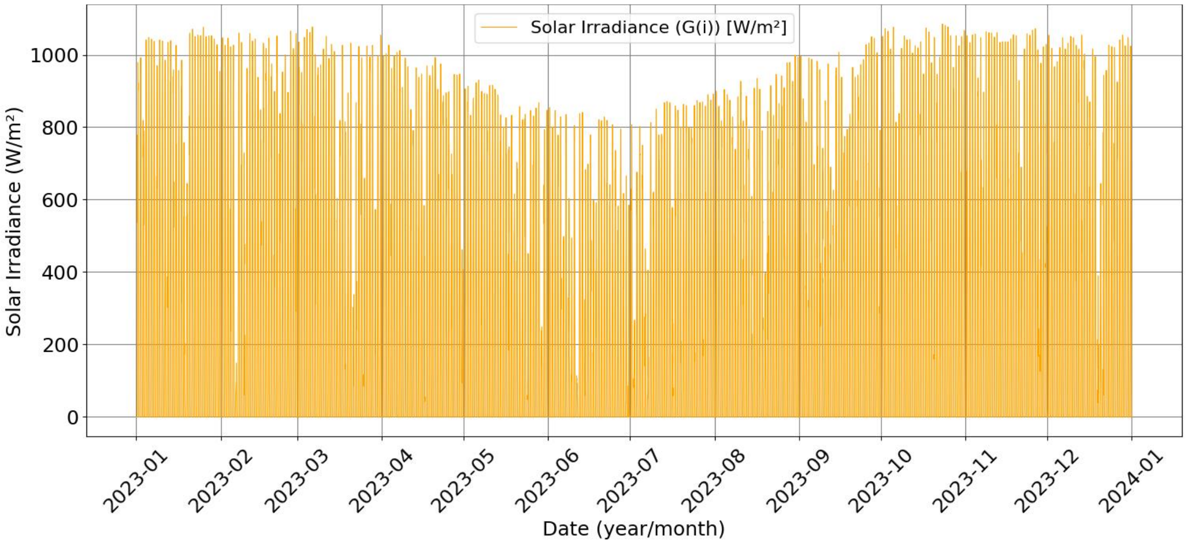

Figure 6: Hourly solar irradiance profile for Recife, Brazil (2023).

Using the irradiance data, the electrolyzer's I-V curve is obtained for each hour. The optimization algorithm seeks the best combination of the number of electrolyzer cells and the electrolyzer temperature to maximize annual hydrogen production. For this purpose, each PSO particle tests a potential combination (N_{cells}, T). It does so by finding the intersection point between the electrolyzer's I-V curve, obtained with these parameters, and the hourly I-V curve of the solar panel. The hourly hydrogen production is calculated for each intersection, and these values are accumulated over the year. From the optimization process, the decision variables that achieves the highest annual production of 1.905 kg of H_2/year are N_{cells} = 7 and T = 80°C.

The influence of the number of cells and temperature near to the optimal operation point was explored. Increasing the number of cells does not invariably lead to higher annual hydrogen production, as it shifts the electrolyzer's I-V curve, altering the operating voltage and current. As shown in Fig. 7a, for a fixed temperature of 80°C and a standard panel I-V curve, the operation point (*V, I*) and hydrogen production for 6, 7 and 8 cells are:

- 6 cells: Operation at (15.4 V, 3.47 A), yielding 1.718 kg of H_2/year.
- 7 cells: Operation at (17.81 V, 3.33 A), yielding 1.905 kg of H_2/year.
- 8 cells: Operation at (19.45 V, 2.68 A), yielding 1.792 kg of H_2/year.

On the other hand, for a fixed number of cells, an increase in temperature changes the slope of the electrolyzer's I-V curve. This results in a higher operating current and a lower voltage, thereby reducing losses. For a system with 7 cells under standard panel conditions, the effect of temperature in the operation point and hydrogen production is shown in Fig. 7b as follows:

- 60°C: Operation at (18.65 V, 3.13 A), yielding 1.812 kg of H_2/year.
- 70°C: Operation at (18.25 V, 3.25 A), yielding 1.863 kg of H_2/year.
- 80°C: Operation at (17.81 V, 3.33 A), yielding 1.905 kg of H_2/year.

The optimal configuration of 7 cells at 80°C results in an operating point (17.81 V, 3.33 A) that is close to the panel's Maximum Power Point (MPP) of (17.99 V, 3.30 A) under standard conditions. Then, at high irradiances the PV panel will be working near to the MPP delivering energy at the maximum PV efficiency.

It is important to note that for the optimized decision variables, the operation point changes on irradiance. A high irradiance values, the electrolyzer will achieve the maximum values of current and voltage allowed. By decreasing the irradiance, the electrolyzer will operate at moderate values of current and voltage.

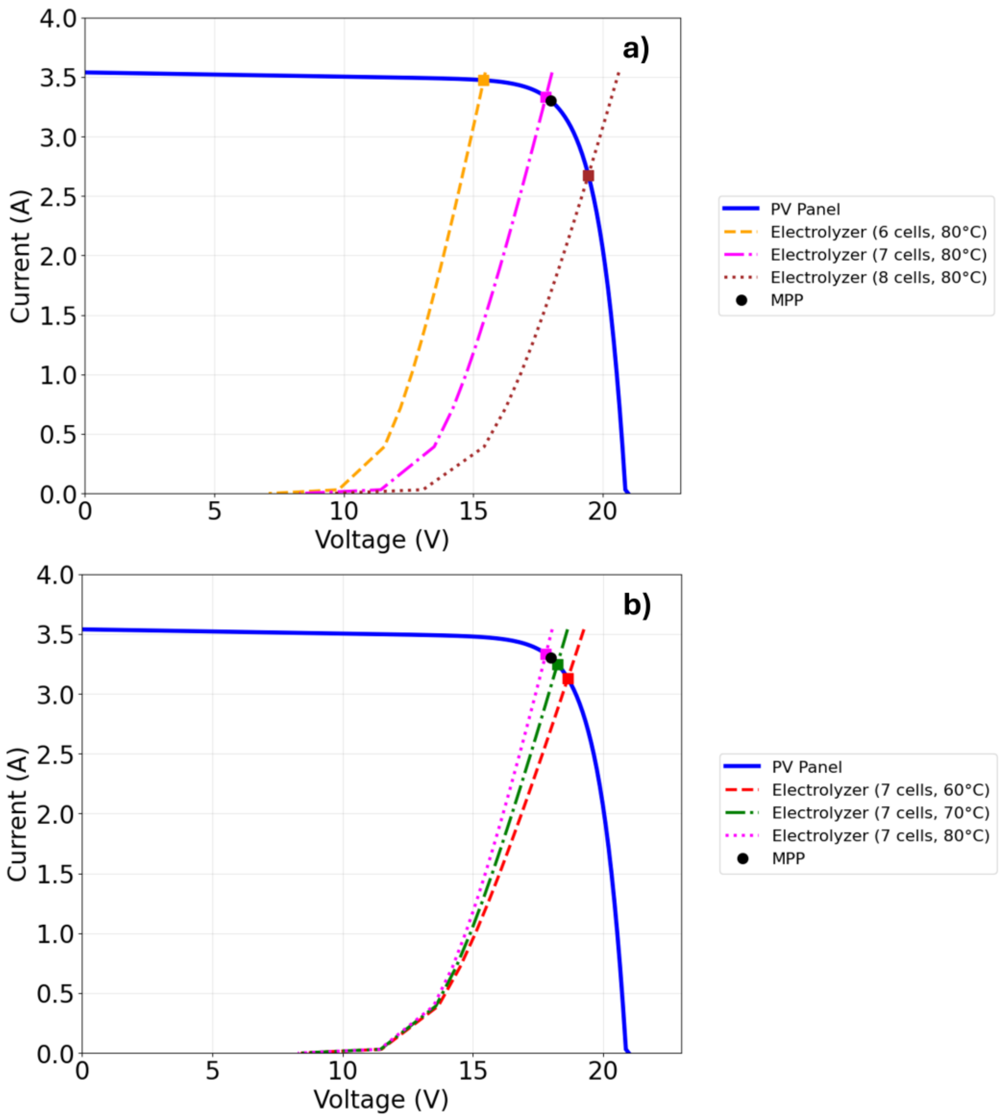

Figure 7: I-V curves of the photovoltaic panel (at standard conditions showing the Maximum Power Point (MPP), filled circle in black) and the electrolyzer for: a) 80ºC and 6, 7 and 8 cells; b) 7 cells at 60ºC, 70ºC and 80ºC.

4. Conclusions

The simulations reveal that an increase in temperature causes the electrolyzer's I-V curve slope to steepen, shifting the curve toward the left, while a temperature decrease reduces the slope, shifting the curve toward the right. Conversely, reducing the number of electrolyzer cells shifts the electrolyzer's I-V curve leftward, while increasing the number of cells shifts it rightward. Therefore, through optimization, it was possible to find the point that provides the maximum hydrogen production by adjusting these two variables (N_{cells}, T). The optimization results demonstrate that: the maximum hydrogen production does not necessarily coincide with the operation point at the MPP of the PV panel at high irradiance, but its very close at standard conditions; that higher temperatures favor hydrogen production since leftward-shifted I-V electrolyzer curves reach higher current levels; and increasing the cell count shifts the I-V curve rightward, leading to reduced current levels, but simultaneously increasing hydrogen production. However, overall system efficiency must be considered when employing a temperature controller to maximize production, as energy consumption increases with the deviation of the electrolyzer's temperature from its optimal temperature. High temperatures also accelerate electrode degradation, which can increase the overall system maintenance costs. Furthermore, when modeling the PV-electrolyzer system, it is necessary to consider that operating voltages higher than the typical range (~2.2 V) can lead to system efficiency losses, electrolyzer degradation, and reduced safety. The appropriate selection of the solar panel is a crucial step to maximize production while meeting project requirements. In addition to technical aspects, economic factors must also be evaluated to determine the optimal size and operation point of the PV panel and electrolyzer.

5. Acknowledgments

For financial support and research incentives, the authors would like to thank the Science and Technology Foundation of Pernambuco/ Fundação de Amparo à Ciência e Tecnologia de Pernambuco (FACEPE, Grant Number APQ-2274-3.14/24). This work is part of the Institute of Science, Technology and Innovation of Pernambuco (IPECTI) - Renewable Energies and Decarbonization (Zero C Network) / Instituto Pernambucano de Ciência, Tecnologia e Inovação (IPECTI) em Energias Renováveis e Descarbonização (Rede Zero C). Also, the authors would like to thank the Coordenação de Aperfeiçoamento de Pessoal de Níıvel Superior-Brazil (CAPES) under Grant 001 and Conselho Nacional de Desenvolvimento Científico e Tecnológico (CNPq)-Brazilian Agencies (FACEPE BPP-0075-3.05/24).

6. References

Amores, E., Rodríguez, J., Carreras, C., 2014. Influence of operation parameters in the modeling of alkaline water electrolyzers for hydrogen production. International Journal of Hydrogen Energy 39, 13063-13078.

Baquero, J. E. G., Monsalve, D. B., 2024. From fossil fuel energy to hydrogen energy: Transformation of fossil fuel energy economies into hydrogen economies through social entrepreneurship. International Journal of Hydrogen Energy 54, 574-585.

Bussieck, M., Pruessner, A., 2003. Mixed-integer nonlinear programming. SIAG/OPT Newsletter: Views & News 14, 19-22.

Daoudi, C., Bounahmidi, T., 2024. Overview of alkaline water electrolysis modeling. International Journal of Hydrogen Energy 49, 646-667.

EL-SHAFIE, M., 2023. Hydrogen production by water electrolysis technologies: A review. Results in Engineering 20, 101426.

Emam, A. S., Hamdan, M.O., Abu-Nabah, B.A., Elnajjar, E., 2024. Enhancing alkaline water electrolysis through innovative approaches and parametric study. International Journal of Hydrogen Energy 55, 1161-1173.

Fukuyama, Y., 2008. Fundamentals of particle swarm optimization techniques, in: Lee, K.Y., El-Sharkawi, M.A. (Eds.), Modern Heuristic Optimization Techniques: Theory and Applications to Power Systems. Wiley, Hoboken, 71-87.

Gad, A.G., 2022. Particle swarm optimization algorithm and its applications: a systematic review. Archives of Computational Methods in Engineering 29, 2531-2561.

Hu, K., Fang, J., Ai, X., Huang, D., Zhong, Z., Yang, X., Wang, L, 2022. Comparative study of alkaline water electrolysis, proton exchange membrane water electrolysis and solid oxide electrolysis through multiphysics modeling. Applied Energy 312, 118788.

International Energy Agency (IEA), 2025. Electricity 2025: Analysis and Forecast to 2027. International Energy Agency, Paris.

International Energy Agency (IEA), 2024. Global Hydrogen Review 2024. International Energy Agency, Paris.

Incer-Valverde, J., Korayem, A., Tsatsaronis, G., Morosuk, T., 2023. "Colors" of hydrogen: Definitions and carbon intensity. Energy Conversion and Management 291, 117294.

Jin, L., Nakashima, R. N., Comodi, G., Frandsen, H. L., 2025. Alkaline electrolysis for green hydrogen production: A novel, simple model for thermo-electrochemical coupled system analysis. Applied Thermal Engineering 262, 125154.

Kovač, A., Paranos, M., Marciuš, D., 2021. Hydrogen in energy transition: A review. International Journal of Hydrogen Energy 46, 10016-10035.

Kumar, S. S., Lim, H., 2022. An overview of water electrolysis technologies for green hydrogen production. Energy Reports 8, 13793-13813.

Stewart, K., Lair, L., De La Torre, B., Phan, N. L., Das, R., Gonzalez, D.,Yang, Y., 2021. Modeling and optimization of an alkaline water electrolysis for hydrogen production, in: 2021 IEEE Green Energy and Smart

Systems Conference (IGESSC). IEEE, Long Beach, pp. 1-6.
Tian, H., Mancilla-David, F., Ellis, K., Muljadi, E., Jenkins, P., 2012. A cell-to-module-to-array detailed model for photovoltaic panels. Solar Energy 86, 2695-2706.
Ulleberg, Ø., 2003. Modeling of advanced alkaline electrolyzers: a system simulation approach. International Journal of Hydrogen Energy 28, 21-33.
Yang, X., 2008. Introduction to Mathematical Optimization: From Linear Programming to Metaheuristics.

7. Web References

Ameresco,Inc.,(2015). *Ameresco Solar 60J / 60W Product Datasheet*. Available at: https://www.amerescosolar.com/wp-content/uploads/Ameresco-Solar-60J-60W_1.pdf (Accessed: October 20, 2025).
ElectroCell,(2017). *Micro Flow Cell* - Technical Data (V1_2017). Available at: https://cdn.prod.website-files.com/679c956c70cb321a0d925e2e/67a1e3bf8bcf4410fe599e4e_micro-flow-cell_technical-data.pdf (Accessed: October 20, 2025).
European Commission,(2025). *PVGIS - Photovoltaic Geographical Information System*. Available at: https://re.jrc.ec.europa.eu/pvg_tools/en/ (Accessed: March 6, 2025).
Rohatgi, A.,(2024). *WebPlotDigitizer*. Available at: https://automeris.io/ (Accessed: October 21, 2025).